

Chapter 2

Literature Review

2.1 Cathode materials for SOFCs

Primarily, the cathode provides the reaction sites for the electrochemical reduction of the oxidant. Therefore, the cathode materials largely play an important role on the performance of SOFCs. The crucial required properties for specific cathode materials are summarized.

The cathode must offer such high stability in oxidizing atmosphere. Chemical properties, phase, morphology and dimension should not change during operation since these can reduce the cell performance. In order to support the oxygen reduction, the cathode must possess high electronic conductivity and sufficient catalytic activity at operating temperature. Adequate porosity is also required to allow gas transport to the reaction sites. Furthermore, cathode must have chemical and thermal expansion compatible with the adjacent components, especially electrolyte material, to avoid cracking and delamination during thermal cycling. Other desirable properties for the cathode are good strength, moderate cost and easy fabrication.

The high operating temperature of SOFCs and the highly oxidizing atmosphere at cathode suggest that only noble metals or electronic conducting oxides can be used as cathode materials. Early SOFCs used noble metals such as platinum, palladium or silver as they possess high electronic conductivity^(1,3). However, they are not suitable for use in practical SOFCs due to their cost and, particularly silver, the instability for a long term operation at high temperature. Some oxides belong to the perovskite family (ABO_3) are suitably used as SOFC cathodes. Nevertheless, the requirements for similar thermal expansion coefficient behavior and chemical compatibility with the solid electrolyte based on yttria-stabilized zirconia (YSZ) tend to restrict the choice of applicable oxides. One perovskite which is commonly used as a cathode material in SOFCs is doped $LaMnO_3$ ⁽¹⁻³⁾. In order to enhance the electrical conductivity, $LaMnO_3$ has been partially substituted with various lower valence ions on either A or B sites such as barium, calcium, chromium, copper, lead, magnesium and

nickel⁽¹⁾. Presently, strontium-doped LaMnO_3 is the most successful cathode for SOFCs using YSZ electrolyte because of its high electronic conductivity, high catalytic activity for oxygen reduction, chemical and thermal compatibility with YSZ electrolyte^(1,3,7).

2.2 Lanthanum Strontium Manganite ($\text{La}_{1-x}\text{Sr}_x\text{MnO}_3$)

The operation of cathode is carried out in oxidizing atmosphere at high temperature; hence, many properties at the operating condition of cathode such as crystal structure, nonstoichiometry of materials, electrical conductivity, thermal expansion, stability and chemical compatibility with YSZ electrolyte must be concerned.

2.2.1 General properties and crystal structure

LaMnO_3 is a perovskite oxide of general formula ABO_3 where A and B sites are occupied by trivalent rare earth cation and trivalent transition metal, respectively. The phase diagram⁽¹⁾ of La_2O_3 - Mn_2O_3 is shown in Fig.2.1. 50 mol% La, LaMnO_3 shows perovskite phase. The melting point is approximately 2153 K⁽¹⁾.

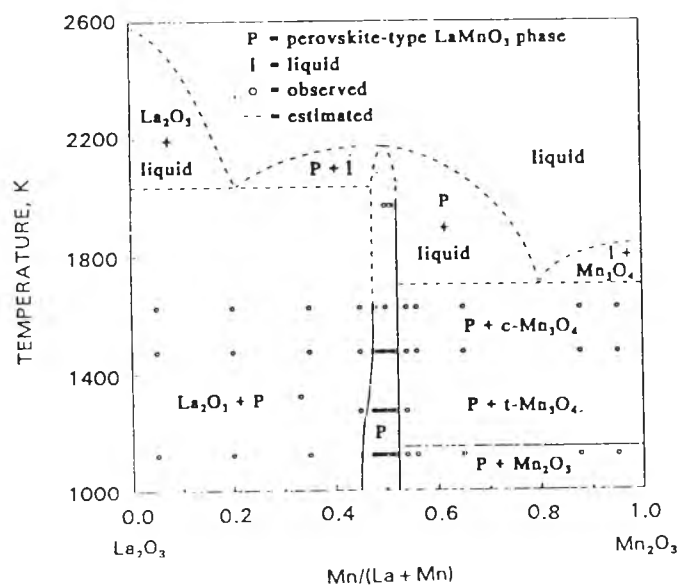


Fig.2.1 Phase diagram of La_2O_3 - Mn_2O_3 system⁽¹⁾

The ideal structure of LaMnO_3 oxide is cubic, as shown in Fig.2.2. The La cation is at the body center and it is surrounded by eight Mn cations at the unit cell corners. The Mn cation is six-fold co-ordinated by oxygen ions forming octahedral $\text{MnO}_{6/2}$ framework and the La cation is twelve fold dodecahedrally co-ordinated by oxygen ions.

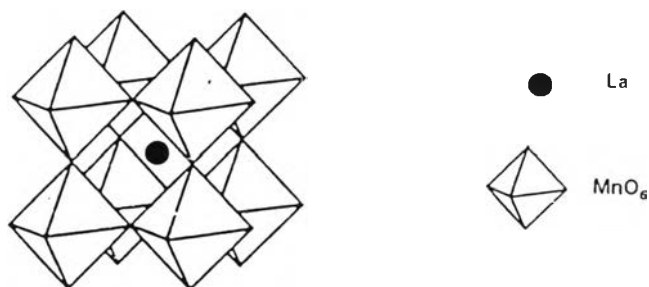


Fig.2.2 Ideal perovskite structure of LaMnO_3 ⁽¹⁾

This ideal cubic structure may undergo atomic distortion leading to orthorhombic or rhombohedral structure. The crystal structure of LaMnO_3 depends on the Mn^{4+} ion content in the lattice, which is sensitive to the degree of oxygen nonstoichiometry⁽¹⁾. Nakamura et al.⁽⁸⁾ reported that the stoichiometric LaMnO_3 displayed the orthorhombic structure with $a = 5.535 \text{ \AA}$, $b = 5.7434 \text{ \AA}$ and $c = 7.693 \text{ \AA}$.

Stoichiometric LaMnO_3 crystallized in the orthorhombic structure at room temperature and transformed to rhombohedral structure at 600°C ^(1,9). However, various transformation temperatures were reported for LaMnO_3 samples having different degree of oxygen nonstoichiometry^(1,3). For nonstoichiometric LaMnO_3 , the crystal structure can undergo a phase transformation from orthorhombic or rhombohedral to cubic structure by increasing Mn^{4+} content or high oxygen excess because the oxidation of Mn^{3+} to smaller Mn^{4+} ions results in the less distorted cubic structure^(1,10). For example, LaMnO_3 with 28% Mn^{4+} was reported to be rhombohedral structure which had lattice parameters of $a = 5.5318 \text{ \AA}$ and $\alpha = 60.615^\circ$ ⁽¹⁰⁾.

Doping lower valency of Sr cation also increased Mn^{4+} concentration in LaMnO_3 ^(1,9). Reported by many researchers, LaMnO_3 doped with 16 mol% Sr showed rhombohedral structure⁽¹⁰⁻¹²⁾. Mackor et al.⁽¹¹⁾ reported the lattice parameter of $a = 3.887 \text{ \AA}$ and $\alpha = 90.5^\circ$, which is similar to that reported by Kertesz et al.⁽¹²⁾ in previous study ($a = 3.893 \text{ \AA}$ and $\alpha = 90.49^\circ$). In contrast, Aruna et al.⁽¹⁰⁾ published the different value of rhombohedral lattice parameter with $a = 5.4893 \text{ \AA}$ and $\alpha = 60.41^\circ$. Also, they found that the dimension of rhombohedral unit cell decreased with Sr content because the increasing of smaller Mn^{4+} ions resulted in unit cell contraction. However, in their work, the rhombohedral transformed to cubic phase for the composition containing 44% Mn^{4+} , as Sr content increased up to 30 mol%. This cubic structure has lattice parameter of $a = 7.7611 \text{ \AA}$ ⁽¹⁰⁾. Different from others, Gharbage et al.⁽¹³⁾ observed a monoclinic structure with $a = 5.481 \text{ \AA}$, $b = 5.493 \text{ \AA}$, $c = 7.701 \text{ \AA}$ and $\beta = 90.17^\circ$ in 50 mol% Sr-doped LaMnO_3 . The variety of crystal structure is not only a result from Sr content in this oxide but also the preparation conditions, which were described elsewhere⁽¹⁰⁻¹³⁾.

2.2.2 Nonstoichiometry and stability

At high temperature, LaMnO_3 tended to exhibit a wide range of oxygen nonstoichiometry, depending on firing atmosphere, temperature and time^(1,12). Fig.2.3 showed that the amount of oxygen content in LaMnO_3 varied with oxygen partial pressure and temperature. In oxidizing atmosphere, LaMnO_3 was stable and exhibited oxygen excess or superstoichiometry which was represented by $\text{LaMnO}_{3+\delta}$. As the oxygen partial pressure decreased, this oxygen content decreased and became stoichiometry in a narrow range of oxygen partial pressure. In reducing atmosphere, this oxide exhibited oxygen deficient or substoichiometry which was represented by $\text{LaMnO}_{3-\delta}$. Under extremely low oxygen partial pressure, this oxide became unstable and dissociated into La_2O_3 and MnO ^(1,3). At 1000°C , the lowest oxygen partial pressure before undoped LaMnO_3 decomposed into multiple phases was about 10^{-14} to 10^{-15} atm⁽¹⁾ (10^{-9} to 10^{-10} Pa), so called the critical oxygen partial pressure⁽¹⁾.

Sr-doped LaMnO_3 also displayed various oxygen contents. The level of oxygen excess decreased with increasing Sr dopant, as shown in Fig.2.4⁽¹⁾. Doping

higher Sr content in LaMnO_3 resulted in less stability of this compound⁽¹⁾. Fig.2.5⁽¹⁾ showed that at constant temperature, the critical oxygen partial pressure of Sr-doped LaMnO_3 shifted to higher values as Sr content increased.

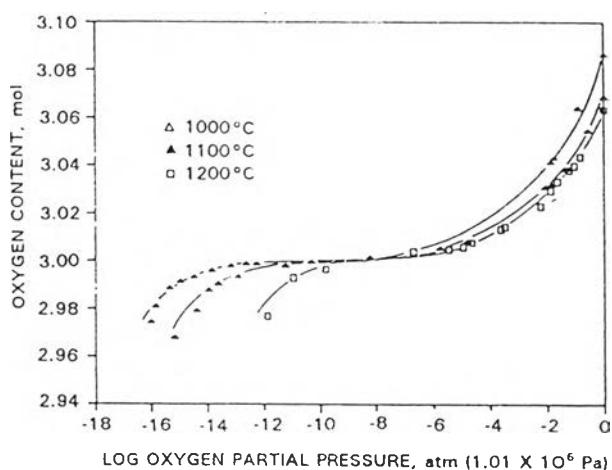


Fig.2.3 Oxygen content of undoped LaMnO_3 as a function of oxygen partial pressure and temperature⁽¹⁾

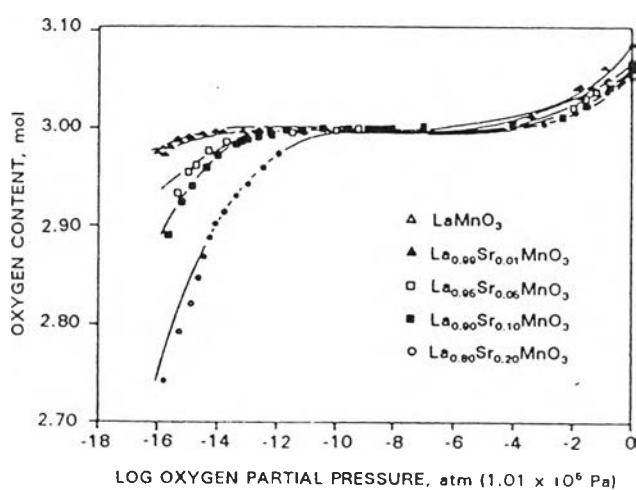


Fig.2.4 Oxygen content of $\text{La}_{1-x}\text{Sr}_x\text{MnO}_3$ as a function of oxygen partial pressure and temperature⁽¹⁾

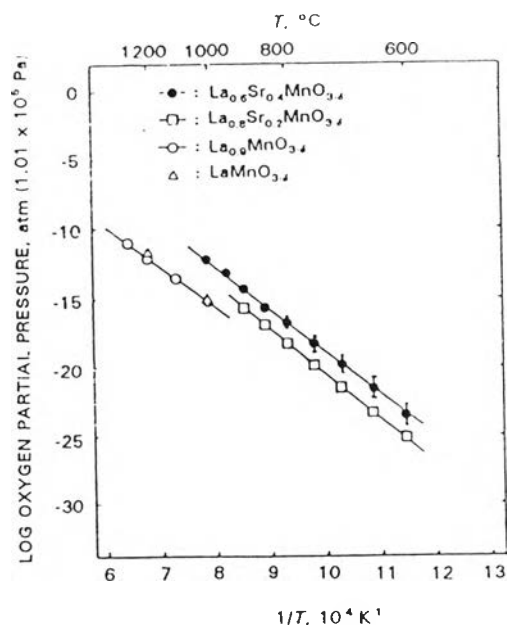


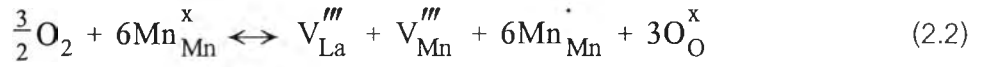
Fig.2.5 Critical oxygen partial pressure of $\text{La}_{1-x}\text{Sr}_x\text{MnO}_3$ ⁽¹⁾

In addition to oxygen nonstoichiometry, LaMnO_3 can also exhibit lanthanum excess or deficiency⁽¹⁾. Lanthanum excess in LaMnO_3 brought about the precipitation of La_2O_3 which tended to form $\text{La}(\text{OH})_3$ ⁽¹⁾. This hydrated form appeared to disintegrate the structure of the sintered samples. Deficient lanthanum in LaMnO_3 is a more stable form and recommended for cathode preparation in SOFCs. However, the amount of lanthanum deficiency is limited to 10% in order to prevent the formation of second phases such as Mn_3O_4 ⁽¹⁾.

2.2.3 Electrical conductivity

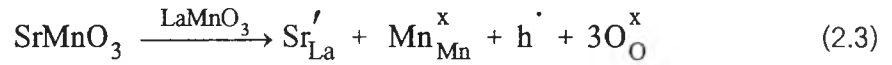
The key feature of an SOFC operation is based on electrical conductivity in ceramic materials, which is related to the concentration of lattice defects.

In oxidizing atmospheres, LaMnO_3 has oxygen excess. Normally, the formation of oxygen interstitial ions in LaMnO_3 perovskite oxide is unexpected due to its close-packed structure. It has been revealed that the oxygen excess in LaMnO_3 could be replaced by the presence of the cation vacancies instead of interstitial oxygen ions^(9,10,14), as expressed by equation (2.1). For example, $\text{LaMnO}_{3.158}$ showed an actual crystallographic formula of $\text{La}_{0.95}\text{Mn}_{0.95}\text{O}_3$ ⁽⁹⁾.



The formation of cation vacancies created holes in order to compensate the electronic charge and simultaneously induce the change in valence state of some manganese ions from Mn^{3+} to Mn^{4+} or a small polaron hopping mechanism expressed by equation (2.2). Therefore, LaMnO_3 is a p-type semiconductor^(1,3,14).

In Sr-doped LaMnO_3 , Sr cation is a divalent substituent for a trivalent La site in perovskite structure. Thus, Sr is called an acceptor dopant. The charge difference of La^{3+} and Sr^{2+} is compensated by the creation of holes or the small polaron hopping⁽¹⁾, illustrated by equation (2.3). As a result, the electronic conductivity increases considerably.



The electrical conductivity depends on many factors, described below.

a) Temperature dependence

The electronic conductivity of Sr-doped LaMnO_3 occurs via a small polaron hopping mechanism, which is thermally activated⁽¹⁴⁾. The temperature dependence of small polaron hopping is generally expressed by Arrhenius equation^(1,14).

$$\sigma = \frac{A}{T} \exp\left(-\frac{E_a}{RT}\right)$$

where σ is the conductivity (S cm^{-1}), T is the temperature (K), E_a is an activation energy for conduction (J mol^{-1}), A is the pre-exponential factor and R is the gas constant ($8.31 \text{ J mol}^{-1} \text{ K}^{-1}$). E_a is obtained from the slope of $\log(\sigma T)$ versus $\frac{1}{T}$.

Fig.2.6⁽¹⁾ showed the electrical conductivity as a function of temperature of both undoped and Sr-doped LaMnO_3 . For undoped LaMnO_3 , the Arrhenius plot showed

a break in conductivity which implied to the phase transformation at this temperature. The electrical conductivity of Sr-doped LaMnO_3 increased with increasing Sr content.

In Fig.2.7. Aruna et al.⁽¹⁰⁾ reported that Sr-doped LaMnO_3 with ≤ 10 mol%Sr showed semiconductor behavior, the resistivity decreased as temperature increased, in all temperature measurements. However, when Sr content ≥ 16 mol%, metallic behavior was observed at low temperature and then changed to semiconductor behavior. The phase transition was also referred in this case.

Lauret et al.⁽¹⁵⁾ reported that Sr-doped LaMnO_3 with 50-55 mol%Sr showed metallic type conduction and with 80 mol%Sr showed semiconductor type conduction.

b) Strontium content dependence

Mackor et al.⁽¹¹⁾ reported that the electrical conductivities at 1000°C of $\text{La}_{1-x}\text{Sr}_x\text{MnO}_3$ increased from 170 to 290 S cm^{-1} when x increased from 0.16 to 0.50. Roosmalen et al.⁽¹⁶⁾ found that the electrical conductivities at 1223 K (950°C) were 115, 175, 265 and 300 S cm^{-1} for x = 0, 0.15, 0.30 and 0.50, respectively. These results were in good agreement with the value of 190 S cm^{-1} at 1273K (1000°C) for x = 0.16 which was estimated by Kertesz et al.⁽¹²⁾.

Lauret et al.⁽¹⁵⁾ studied the conductivity of this composition with x ≥ 0.5 . They reported that the maximum conductivity can be obtained for x = 0.55 and strongly decreased as increasing x from 0.55 to 0.80.

Aruna et al.⁽¹⁰⁾ found that the highest conductivity was limited at x = 0.16. Its value was 202 S cm^{-1} , which was higher than other studies. However, an increasing amount of Sr tended to decrease the conductivity value. They suggested that this might be the effect of Sr on the microstructure of this material. Similarly, this suggestion agreed with that of Roosmalen et al.⁽¹⁶⁾ and Wiik et al.⁽¹⁷⁾ stating that the sinterability or densification of $\text{La}_{1-x}\text{Sr}_x\text{MnO}_3$ decreased as Sr increased.

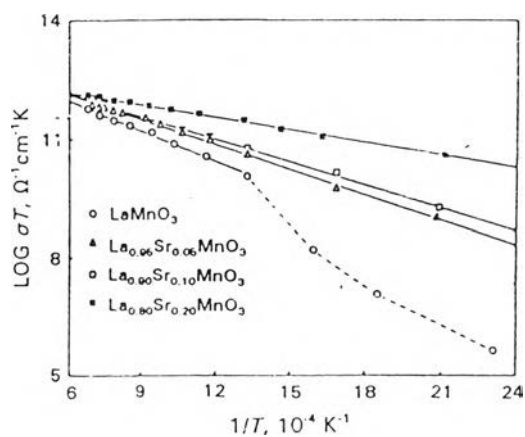


Fig.2.6 Electrical conductivity of undoped and Sr-doped LaMnO_3 ⁽¹⁾

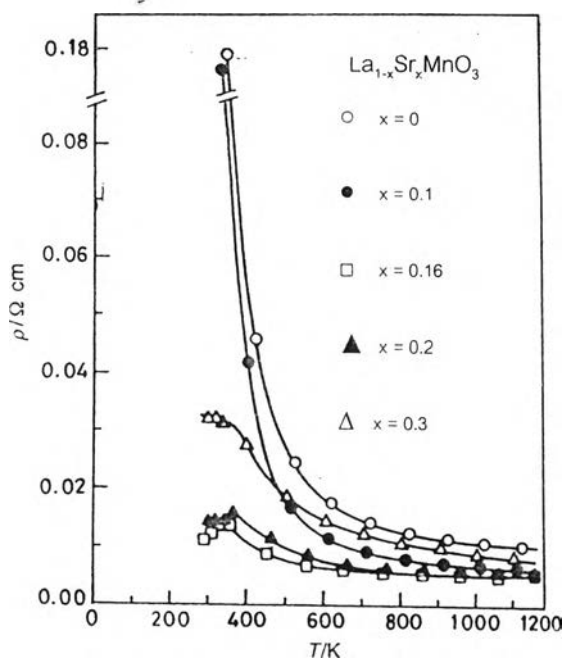


Fig.2.7 Resistivity as a function of temperature of undoped and Sr-doped LaMnO_3 ⁽¹⁰⁾

In addition to the electrical conductivity, Sr content also changed the activation energy. Both of Sr-doped LaMnO_3 were summarized in Table 2.1.

Table 2.1 Electrical conductivity (σ) and activation energy (E_a) of Sr-doped LaMnO_3

Composition	Temperature ($^{\circ}\text{C}$)	σ (S cm^{-1})	E_a (kJ mol^{-1})	Reference
LaMnO_3	900	103	15.80	10
	950	115	-	16
$\text{La}_{0.9}\text{Sr}_{0.1}\text{MnO}_3$	900	116	14.93	10
$\text{La}_{0.85}\text{Sr}_{0.15}\text{MnO}_3$	950	175	-	16
$\text{La}_{0.84}\text{Sr}_{0.16}\text{MnO}_3$	900	202	8.10	10
	1000	170	10.70	11
	1000	190	9.60	12
$\text{La}_{0.8}\text{Sr}_{0.2}\text{MnO}_3$	900	155	8.67	10
$\text{La}_{0.7}\text{Sr}_{0.3}\text{MnO}_3$	900	144	9.63	10
	950	265	-	16
$\text{La}_{0.5}\text{Sr}_{0.5}\text{MnO}_3$	950	300	-	16
	1000	290	4.50	11

c) Oxygen partial pressure dependence

At high oxygen partial pressure, the conductivity of undoped and Sr -doped LaMnO_3 is nearly independent of the variation of oxygen partial pressure. But at low partial pressure of oxygen, the conductivity decreases significantly⁽¹⁾.

In the experiment of Yasuda et al.⁽¹⁸⁾, Fig.2.8 showed that the conductivity of Sr-doped LaMnO_3 was relatively constant in the range of high oxygen partial pressure, $>10^{-8}$ atm. However, below this atmosphere, it decreased exponentially with decreasing the oxygen partial pressure. This can be explained by the transition from electronic to ionic charge compensation, which is attributed to the formation of Mn^{4+} at high oxygen partial pressure and the existence of oxygen vacancies at low oxygen partial pressure. The large amount of dopant brought about the higher conductivity in high oxygen partial pressure region; however, its value dropped abruptly at higher oxygen partial pressure. In other words, the lower Sr content exhibited higher conductivity in low oxygen partial pressure region.

The effect of temperature on the oxygen partial pressure dependence of conductivity was also studied⁽⁸⁾, as shown in Fig.2.9. At the higher temperature, the conductivity of $\text{La}_{0.8}\text{Sr}_{0.2}\text{MnO}_3$ started decreasing at the higher oxygen partial pressure.

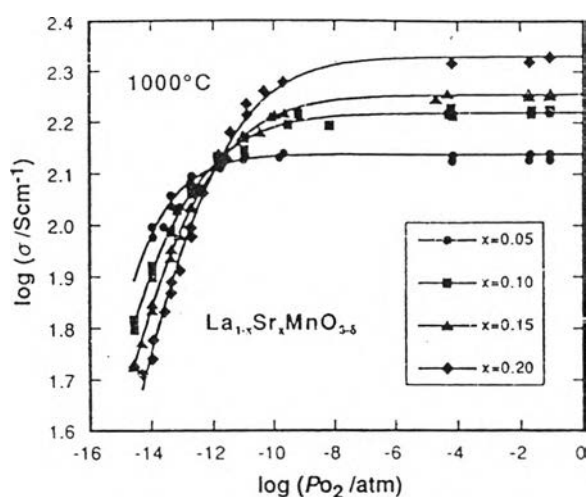


Fig.2.8 Electrical conductivity of $\text{La}_{1-x}\text{Sr}_x\text{MnO}_3$ at 1000°C as a function of oxygen partial pressure⁽⁸⁾

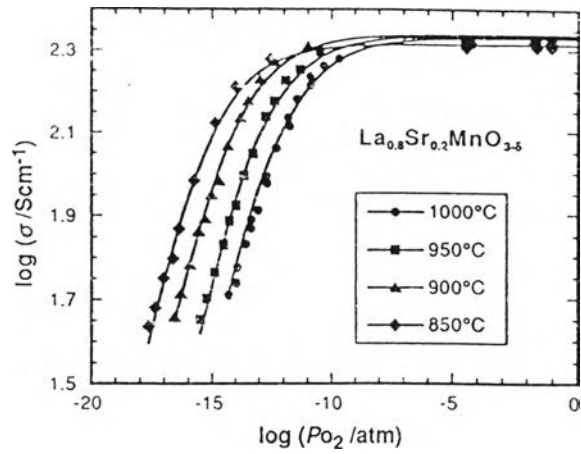


Fig.2.9 Electrical conductivity of $\text{La}_{0.8}\text{Sr}_{0.2}\text{MnO}_3$ as a function of oxygen partial pressure at different temperature measurement⁽⁸⁾

2.2.4 Thermal expansion coefficient

The thermal expansion coefficient from 25°C to 1100°C of undoped LaMnO_3 is about $11.2 \times 10^{-6} \text{ K}^{-1(1,3)}$. This value was slightly higher than that of YSZ (8 mol% Ytria), $10.5 \times 10^{-6} \text{ K}^{-1(7)}$. As Sr content increased, the thermal expansion of Sr-doped LaMnO_3 increased. The thermal expansion coefficients of undoped and Sr-doped LaMnO_3 are also given in Table 2.2.

Table 2.2 The thermal expansion coefficient (TEC) of $\text{La}_{1-x}\text{Sr}_x\text{MnO}_3$

Composition	Temperature ($^{\circ}\text{C}$)	TEC (K^{-1}) $\times 10^{-6}$	Reference
LaMnO_3	25-1100	11.20	1,3
	25-900	11.33	10
$\text{La}_{0.9}\text{Sr}_{0.1}\text{MnO}_3$	25-900	12.18	10
$\text{La}_{0.84}\text{Sr}_{0.16}\text{MnO}_3$	25-900	12.63	10
	20-1000	11.90	11
$\text{La}_{0.8}\text{Sr}_{0.2}\text{MnO}_3$	25-900	13.13	10
$\text{La}_{0.7}\text{Sr}_{0.3}\text{MnO}_3$	25-900	13.74	10

2.5 Interface Reaction

Manganese cations have high mobility at high temperatures and can easily diffuse into the YSZ electrolyte^(1,3), resulting in lanthanum excess at the LaMnO_3 /YSZ interface. The formation of $\text{La}_2\text{Zr}_2\text{O}_7$ insulating layer⁽¹⁾ possibly occurs from a reaction of excess lanthanum and YSZ but it can be suppressed by doping small amount of Sr into LaMnO_3 . Nevertheless, if the amount of Sr dopant increases, SrZrO_3 is possibly formed as another reaction product. Both $\text{La}_2\text{Zr}_2\text{O}_7$ and SrZrO_3 tend to degrade the cell performance because they not only behave like insulating layers but also induce thermal stress at the interface. The electrical conductivities of $\text{La}_2\text{Zr}_2\text{O}_7$ and SrZrO_3 are much lower than that of YSZ and the thermal expansion coefficient from room temperature to 1000°C of $\text{La}_2\text{Zr}_2\text{O}_7$ was reported about $7 \times 10^{-6} \text{ K}^{-1(19)}$, which was, in fact, different from that of YSZ and LaMnO_3 .

The interaction between LaMnO_3 and YSZ at high temperature had been studied by mixing LaMnO_3 and YSZ powder, pressing to form samples, and then firing

to promote reaction at different temperature and time^(17,20). It was found that the formation of second phases, $\text{La}_2\text{Zr}_2\text{O}_7$ and SrZrO_3 , depending on the composition of cathode, firing temperature and firing time.

Stochniol et al.⁽¹⁹⁾ suggested that after firing at 1470 K ($\sim 1200^\circ\text{C}$) for 400 hours, $\text{La}_{1-x}\text{Sr}_x\text{MnO}_3$ ($x < 0.3$) reacted with YSZ, forming $\text{La}_2\text{Zr}_2\text{O}_7$ and the amount of $\text{La}_2\text{Zr}_2\text{O}_7$ decreased as x increased. Nevertheless, when $x > 0.3$, SrZrO_3 was observed as a second phase and its amount increased as x increased. For $x=0.3$, none or few reaction products were formed. However, when it was sintered at higher temperature, 1670 K (1400°C) for 400 hours, $\text{La}_2\text{Zr}_2\text{O}_7$ and SrZrO_3 possibly existed.

Wiik et al. also found that the amount of second phases, $\text{La}_2\text{Zr}_2\text{O}_7$ and SrZrO_3 , tended to increase as the sintering temperature raised from 1200°C to 1350°C for nearly all compositions except $\text{La}_{0.7}\text{Sr}_{0.3}\text{MnO}_3$ in which the amount of both second phases were persistent. At constant temperature, $\text{La}_2\text{Zr}_2\text{O}_7$ content increased with firing time, while SrZrO_3 content was relatively unchanged.

In addition to Sr substitution in La sites, LaMnO_3 with La-deficiency was also recommended to improve the chemical compatibility with YSZ. Stochniol et al.⁽¹⁹⁾ found that a second phase could not be detected in $\text{La}_{0.95-x}\text{Sr}_x\text{MnO}_3$, for $x = 0.3$ when it was sintered at 1470 K for 400 hours or even at 1670 K for 200 hours.

As mentioned previously, it can be concluded that Sr- LaMnO_3 with 30%mol Sr exhibited the best chemical compatibility with YSZ at high temperature. Furthermore, introducing La deficiency and appropriate amount of Sr dopant in LaMnO_3 can slow down the formation of $\text{La}_2\text{Zr}_2\text{O}_7$ and SrZrO_3 at $\text{LaMnO}_3/\text{YSZ}$ interface.